Journal of Power Sources, 43–44 (1993) 27–35

Lithium electrode cycleability and morphology dependence on current density

Masayasu Arakawa, Shin-ichi Tobishima, Yasue Nemoto, Masahiro Ichimura
NTT Interdisciplinary Research Laboratories, Tokai-mura, Ibaraki-ken 319-11 (Japan)

Jun-ichi Yamaki
Advanced Energy Technologies Inc., 3958 Myrtle Street, Burnaby, BC V5C 4G2 (Canada)

Abstract

It is known that the cycleability of lithium secondary batteries depends on both charge and discharge current densities. This paper investigates the cycle life and lithium morphology dependence on charge and discharge current densities. The amount of needle-like lithium increases with decreases in discharge current density.The morphology of the needle-like lithium leads to the formation of 'dead lithium' which plays no role in charge/discharge cycles. Localized deposition and dissolution may be the reason for 'dead lithium' formation. The decrease in cycle life with the increase in charge current density is also explained by this mechanism. Furthermore, high rate discharge leads to the recombination of isolated lithium which results in cycle life increase.

Introduction

The cycle life dependence of lithium secondary cells on both charge and discharge current densities is well known and has been reported in several papers. The cycle life of Li/MoS_2 increases when the discharge current density increases [1]. Similar trends have been reported for Li/MnO_2 [2, 3] and Li/$Li_{0.5}MnO_y$ [4, 5] cells, although their cathode-active materials, organic electrolytes, capacities, charge current densities and cycling voltage regions are all different. The cycle life dependence on charge current densities has also been reported in Li/MoS_2 and Li/$Li_{0.5}MnO_y$ cells. These results suggest that the cycle life dependence on charge and discharge current densities is caused by Li anode degradation. The mechanism of this degradation, however, is still unclear although the high impedance failure of Li anodes was reported in these earlier works.

The reduction in cycle life caused by anode degradation could be explained in several ways:
(i) electrochemically-active Li reacts with electrolyte to form electrochemically-inactive lithium [6];
(ii) metallic lithium is isolated in passivation film [7];
(iii) electrochemical features of passivation film cause high-impedance failure [1], and
(iv) the occurrence of a 'soft short' [1] or electrical isolation of deposited lithium [8] which is related closely to the morphology of the Li anode.

The authors tried to clarify the Li anode degradation from a morphological point of view in connection with the previous work [8, 9, 10]. In this work, the cycle life

0378-7753/93/$6.00

and Li anode morphology dependence on both charge and discharge current densities are discussed.

Experimental

Morphology observation with scanning electron microscopy (SEM)

Coin-type cells (23 mm diameter and 2 mm thick) were assembled using amorphous V_2O_5 (a-V_2O_5) as the cathode-active material and $LiAsF_6$–ethylene carbonate (EC/2-methyltetrahydrofuran (2-MeTHF) as the electrolyte [11]. These cells were disassembled after several cycles and the morphology of the Li anode was observed using SEM.

In situ observation with optical microscopy

The setup and configuration of a test cell for the *in situ* observation of Li deposition are shown in Fig. 1. Lithium cells were assembled on a glass slide. Lithium was deposited on a Ni cathode. The change in morphology was recorded with a video recorder through an optical microscope and a camera. The video images were then copied onto film with a film recorder. The whole process was conducted in a dry atmosphere and the humidity was less than 1%.

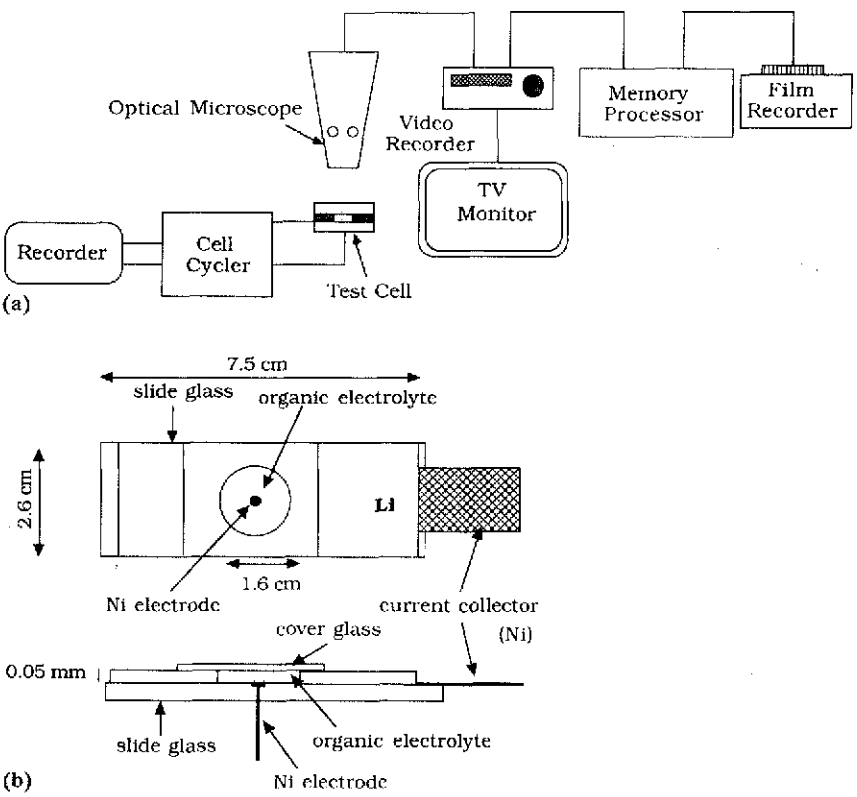

Fig. 1. (a) Setup and (b) cell configuration for *in situ* observation.

Results and discussion

Electrochemically-inactive lithium ('dead lithium') formation

In our previous work, we reported the observation of two types of Li deposited from $LiAsF_6$–EC/2-MeTHF [8]. They were needle-like Li and particle-like Li. The needle-like Li was thought to be 'dead lithium' because it remained on the electrodes after anodic dissolution. The processes of particle-like Li formation and needle-like Li isolation were also proposed as shown in Fig. 2. We believe Li deposition starts with needle-like Li. Particle-like Li grows at the top. In the Li dissolution process, first particle-like Li dissolves followed by needle-like Li. However, heterogeneous dissolution results in Li which is electrically isolated from the electrode.

In situ observation was carried out to verify the proposed mechanism. Needle-like Li showed growth like a proper whisker, which grows from the bottom [12]. Particle-like Li growth was observed at the top of the needle-like Li and at its bending point as shown in Figs. 3 and 4. These results suggest the intimate correspondence with our proposed mechanism.

Change in morphology by varying discharge current density

The cycle life tends to increase with an increase in discharge current density, which is independent of the cathode-active materials, organic electrolytes, cycling capacities, charge current densities and cycling voltage regions, as mentioned previously. The anode morphology was investigated in order to explain the current density dependence on cycle life.

Figure 5 shows the morphology dependence on discharge current density. Li/a-V_2O_5 cells were discharged at 0.2 mA/cm^2 and at 3.0 mA/cm^2. Localized Li stripping occurred at a high discharge rate, but relatively delocalized Li stripping occurred at a high discharge rate. Native surface films on Li foil, which consist probably of Li_2O, Li_3N, Li_2CO_3, etc., and products of the reaction with organic electrolyte, may cause these differences. Namely, current will be focussed in the relatively low impedance part of native films during low rate discharge. This is because the overpotential induced by constant current discharge may not be sufficient for Li to dissolve through the high impedance part of native films. On the other hand, high overpotential which is sufficient

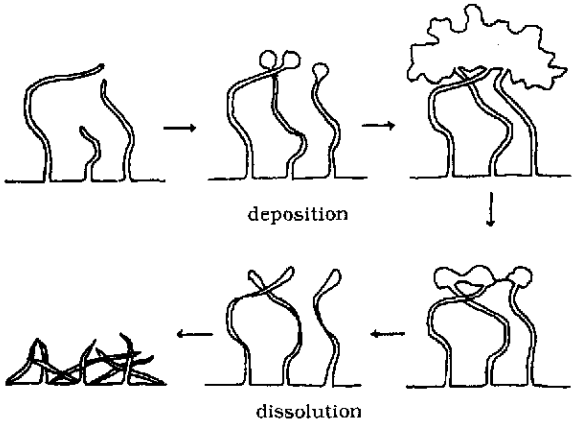

Fig. 2. Proposed mechanism of particle-like lithium formation and needle-like lithium isolation.

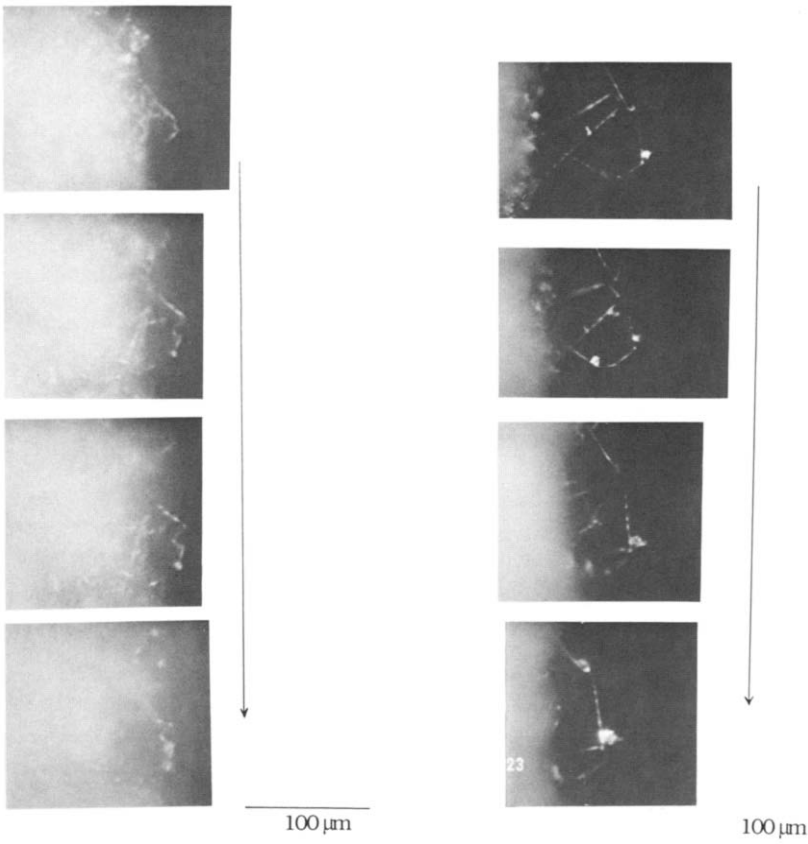

Fig. 3. Photographs of particle-like lithium growth at the top of needle-like lithium.

Fig. 4. Photographs of particle-like lithium growth at the bending point of needle-like lithium.

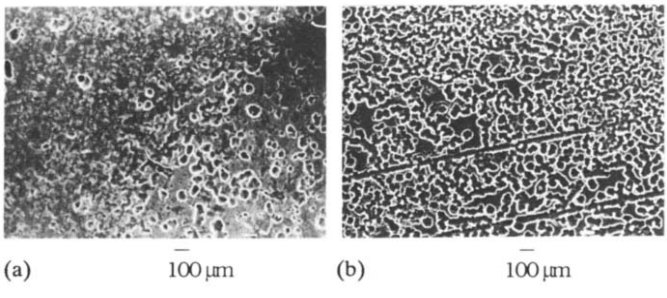

Fig. 5. Morphology dependence on discharge current density: (a) discharged for 9.0 mA h (0.2 mA/cm^2), and (b) discharged for 9.0 mA h (3.0 mA/cm^2).

for the Li to dissolve from all parts of Li anode may be induced by a 3.0 mA/cm^2 discharge.

When the cells were charged at 0.4 mA/cm^2 after discharge, needle-like Li grew in the cell discharged at 0.2 mA/cm^2 as shown in Fig. 6. In contrast, particle-like Li grew in the cell discharged at 3.0 mA/cm^2. In the charging procedure, Li deposition was localized at the point from which Li was dissolved during the discharge. Therefore, the actual charge current density would be higher in the Li anode discharged at 0.2 mA/cm^2 than in that discharged at 3.0 mA/cm^2. The impedance or the passivation film on Li stripped during the discharge may be lower than that of native films. This result suggests that nonuniform stripping during discharge causes the nonuniformity of the charge current density, resulting in the deposition of needle-like Li.

Figure 7 shows Li morphologies after the 5th and 10th discharge. Mossy needle-like Li largely covers the anode in the cell discharged at 0.2 mA/cm^2. On the other hand, no mossy Li was observed in the cell discharged at 3.0 mA/cm^2. This mossy needle-like Li is what was referred to earlier as 'dead lithium' which reduces the cycle life. These results indicate that morphological change is one of the factors which reduces the cycle life at a low discharge current density.

In addition to the homogeneous dissolution resulting in particle-like Li deposition, there is another advantage with high rate discharge. That is the recombination of isolated Li with the electrode during discharge. Figure 8 shows the test cell configuration for *in situ* observation. Isolated Li is positioned between two electrodes. Constant current discharge and charge was provided using this half-cell. Morphological change between the anode and the isolated Li was observed with an optical microscope as before. A 0.5 mA discharge and charge operation was carried out as shown in Fig. 9. Figure 10 shows the growth of Li dendrites from the isolated Li during discharge. The dendrites connect the isolated Li with the Li anode. This phenomenon may occur because of the voltage gradient between the Li anode and the isolated Li. Namely, if there is sufficient voltage gradient, isolated Li would be at the potential of Li deposition. Therefore, high current density discharge also leads to the recombination of isolated Li which in turn results in cycle life increase.

Change in morphology by varying charge current density

The cycle life also tends to increase with a decrease in charge current density, as mentioned above. Figure 11 shows the morphology dependence on charge current

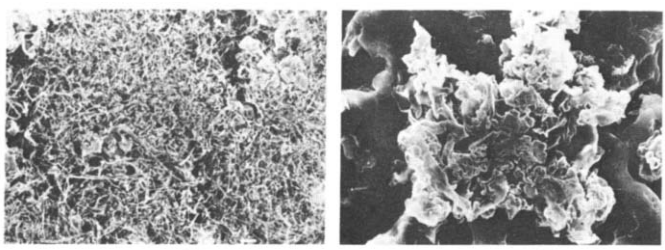

Fig. 6. Influence of discharge current density on morphology during charge: (a) charged for 2.4 mA h at 0.4 mA/cm^2 after being discharged for 9.0 mA h at 0.2 mA/cm^2, and (b) charged for 2.4 mA h at 0.4 mA/cm^2 after being discharged for 9.0 mA h at 3.0 mA/cm^2.

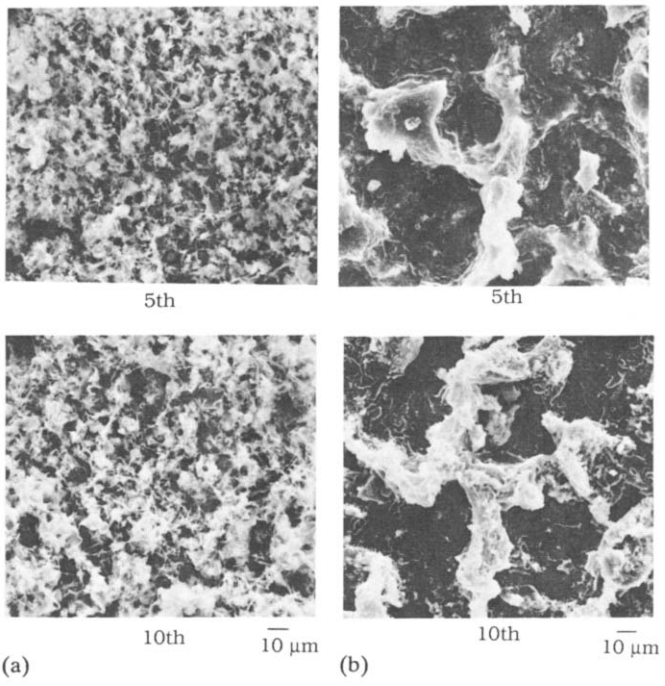

Fig. 7. Morphology of lithium anode after 5th and 10th discharge: (a) discharge current 0.2 mA/cm^2, charge current 0.4 mA/cm^2; (b) discharge current 3.0 mA/cm^2, charge current 0.4 mA/cm^2.

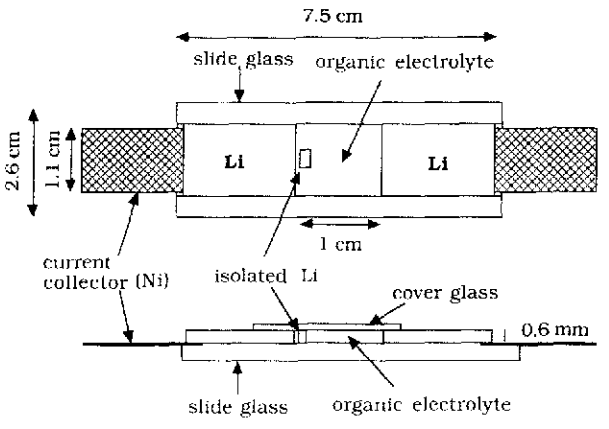

Fig. 8. Test cell configuration for *in situ* observation of the recombination of isolated lithium.

density. Li/a-V_2O_5 cells were discharged at 3.0 mA/cm^2 and then charged at 0.5 and 1.5 mA/cm^2, respectively. Needle-like Li morphology was observed at a high current density. In contrast, particle-like Li was observed at a low current density.

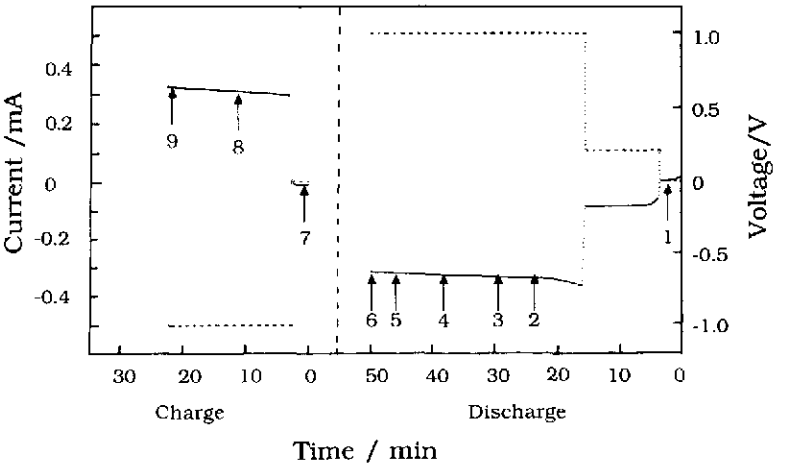

Fig. 9. Profile of voltage and current: (——) voltage, (– – –) current. The numbers in the Fig. show the point of which the photographs in Fig. 10 were taken.

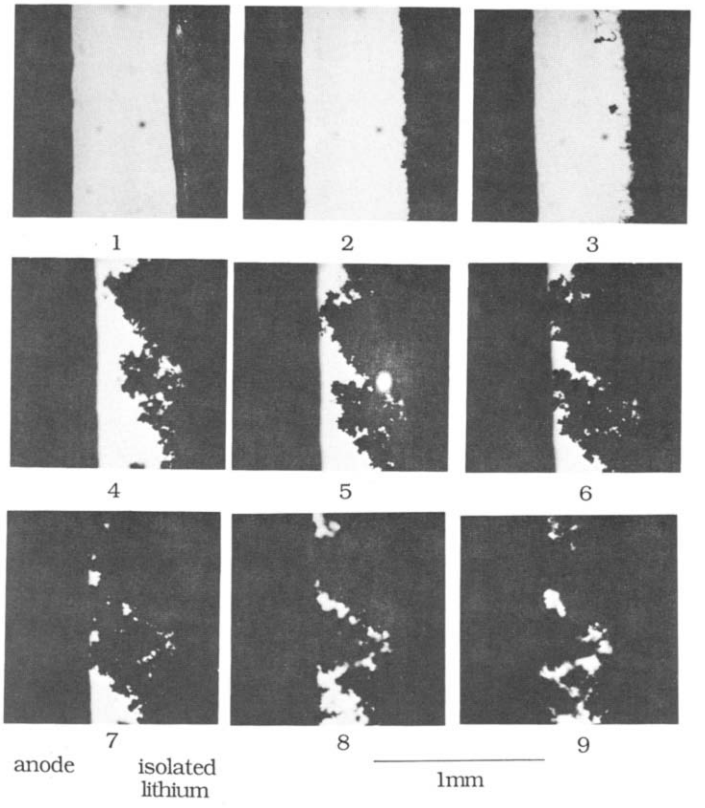

Fig. 10. Recombination of the isolated lithium with the anode, see Fig. 9.

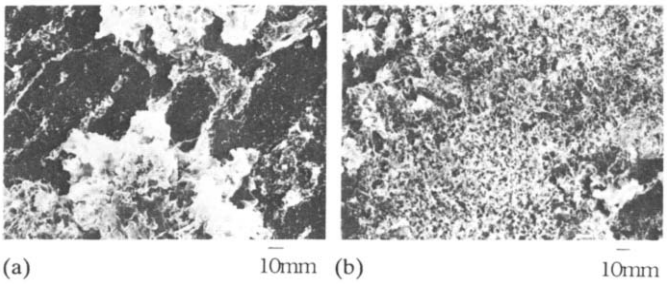

Fig. 11. Morphology dependence on charge current density: (a) charged for 1.5 mA h at 0.5 mA/cm^2 after being discharged for 9.0 mA h at 3.0 mA/cm^2, and (b) charged for 1.5 mA h at 1.5 mA/cm^2 after being discharged for 9.0 mA h at 3.0 mA/cm^2.

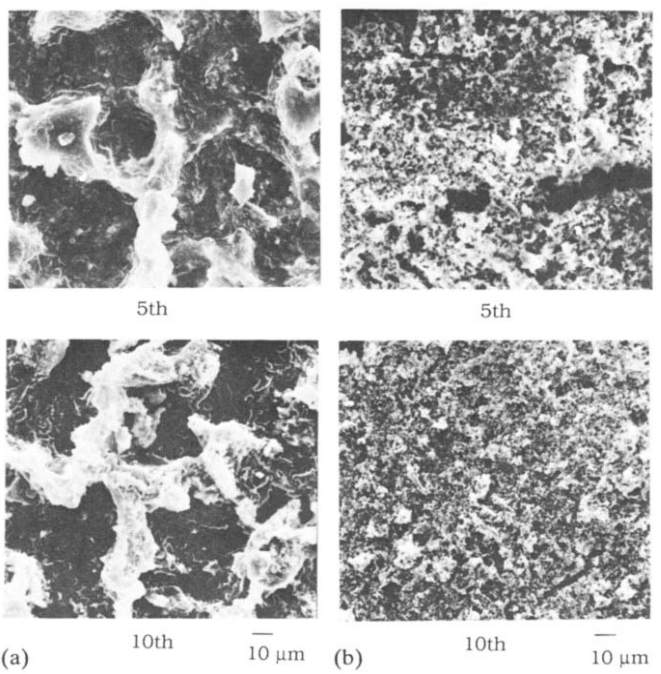

Fig. 12. Morphology of lithium anode after the 5th and 10th discharge: (a) discharge current 3.0 mA/cm^2, charge current 0.4 mA/cm^2; (b) discharge current 3.0 mA/cm^2, charge current 1.5 mA/cm^2.

Needle-like Li gradually covered the Li electrode when the cells were cycled at a high charge rate. Figure 12 shows Li anode morphology after the 5th and 10th discharge at 0.5 and 1.5 mA/cm^2, respectively. The discharge rate was 3.0 mA/cm^2. The decrease in cycle life with an increase in charge current density would thus be explained by the 'dead lithium' formation which was discussed in the section on discharge current density dependence.

Conclusion

Cycle life dependence on both charge and discharge current densities was investigated by studying the morphological change in the Li anode. Needle-like Li deposition which leads to 'dead lithium' formation increases when the discharge current density decreases. A high rate discharge also leads to the recombination of isolated Li resulting in cycle life increase. Needle-like Li deposition increases when the charge current density increases. The results suggest that the morphology of the Li anode is an important factor leading to an understanding of cycle life degradation.

Acknowledgement

The authors wish to thank Mr Nobuo Inagaki, Dr Katsuichi Yotsumoto and Mr Noboru Asano for their helpful guidance and discussions during the course of this work.

References

1 F. C. Lamman and K. Brandt, *J. Power Sources, 24* (1988) 195.
2 K. Brandt and M. Jazkow, *Ext. Abstr., 5th Int. Meet. Lithium Batteries, Beijing, China, 1990,* p. 69.
3 M. W. Jazkow, *Ext. Abstr., Fall Meet. Electrochemical Society, Seattle, WA, USA, 1990,* Vol. 90-2, p. 76.
4 T. Nagaura, Overhead Projection Sheets, *Int. Battery Association Meet., Seattle, WA, USA, 1990,* p. 177.
5 T. Nagaura, *Prog. Batteries Mater., 10* (1991) 208.
6 R. D. Rauh and S. B. Brummer, *Electrochim. Acta, 22* (1977) 75.
7 E. Peled, in J. P. Gabano (ed.), *Lithium Batteries,* Academic Press, New York, 1983, p. 43.
8 I. Yoshimatsu, T. Hirai and J. Yamaki, *J. Electrochem. Soc., 135* (1988) 2422.
9 T. Hirai, I. Yoshimatsu and J. Yamaki, *Ext. Abstr., Spring Meet. Electrochemical Society, Philadelphia, PA, USA, 1987,* Vol. 87-1, p. 706.
10 J. Yamaki, *Ext. Abstr., 5th Int. Meet. Lithium Batteries, Beijing, China, 1990,* p. 50.
11 M. Arakawa, S. Tobishima, T. Hirai and J. Yamaki, *J. Electrochem. Soc., 133* (1986) 1527.
12 S. E. Koonce and S. M. Arnold, *J. Appl. Phys., 24* (1953) 365.